Available online at www.sciencedirect.com
ScienceDirect
Intermetallics 15 (2007) 404–412
Intermetallics
www.elsevier.com/locate/intermet

Porous Ni–Ti ignition and combustion synthesis

C. Zanotti [a,*], P. Giuliani [a], A. Terrosu [a], S. Gennari [b], F. Maglia [b]

[a] Institute for Energetics and Interphases (IENI-CNR), Milano Labs., Via R. Cozzi, 53, I 20125 Milano, Italy
[b] Institute for Energetics and Interphases, Pavia Labs., and Dept. Physical Chemistry, University of Pavia, Viale Taramelli, 16, I 27100 Pavia, Italy

Received 22 June 2006; received in revised form 27 July 2006; accepted 17 August 2006
Available online 25 September 2006

Abstract

The self-propagating high-temperature synthesis of Ni–Ti mixtures was investigated with particular attention to the ignition step. Ignition was performed using an integrated laser diode system which allows fine control of the heating and ignition processes. The experimental parameters controlling the ignition step such as thermal conductivity, surface absorbance, ignition temperature and energy were obtained both experimentally and by numerical simulation as a function of initial stoichiometry, reactants particle size, and heating cycle. Appropriate ignition conditions were searched in order to minimize the thermal gradients inside the pellet obtaining constant reaction temperature and velocity. Dependencies of reaction front velocity and reaction temperature on the pre-heating one were reported too.

Keywords: A. Intermetallics, miscellaneous; C. Powder metallurgy; C. Reaction synthesis; G. Biomedical applications

1. Introduction

Shape memory alloys (SMAs) constitute a large group of alloys with unique properties, that allow technological applications in various fields [1]. In the last two decades, researches concerning this kind of materials have been significantly advanced and oriented both to more basic aspects (such as the theoretical modelling and understanding of their martensitic transformation [2] and the structure and substructure formation of various alloys [3]), and to more technological aspects, such as to the discovery of new SMAs and their applications [4], and to the possible preparation procedures of these materials [5].

Among SMAs, NiTi has been extensively investigated thanks to its excellent mechanical properties (ductility, impact resistance and damping), its good corrosion resistance, its high biocompatibility (which make it an ideal candidate for use in bone implants), as well as for its remarkable shape memory features [6–9]. This alloy has been shown to be commercially important for its potential use as a functional material in many engineering applications, including couplings, actuators, smart materials, as well as external and internal biomedical applications, such as orthodontic arch wires, catheters, and orthopaedic implants [4,10,11].

Porous NiTi SMA is another promising candidate for biomedical applications, but has been acknowledged as very important for use in bone implants only very recently and has hence been subject of fewer studies in literature. Apart from the usual characteristics of SMAs (good mechanical properties, corrosion resistance, high biocompatibility, pseudoelasticity, shape as well as volume memory effect [6]), NiTi in its porous structure allows the ingrowth of new-bone tissue along with the transport of body fluids, thus ensuring a harmonious bond between the implant and the body [6]. Moreover, the possibility to control the porosity during the production process can lead to an adjustable elastic modulus of the final product and hence to a better matching with the elastic modulus of the human bones [12–15].

The potential application and the commercial development of NiTi alloys have, however, been limited by the difficulties and costs of the synthesis, and by the machining of the final product. Conventional routes for the production of NiTi for

* Corresponding author. Tel.: +39 02 66173 310; fax: +39 02 66173 307.
E-mail address: zanotti@ieni.cnr.it (C. Zanotti).

0966-9795/$ - see front matter © 2006 Published by Elsevier Ltd.
doi:10.1016/j.intermet.2006.08.002

shape memory effect consist in the synthesis of the alloy starting from pure elemental metals. This is normally performed either by vacuum induction melting (VIM) or by vacuum arc re-melting (VAR). Subsequently, the product undergoes hot-working and forming to obtain the final desired shape [16]. It is worth noting that the processes above are characterized by the extreme reactivity of the melt and, being "relatively" slow, by a certain degree of segregation in the final material, due to the difference in density of the two reacting metals ($\rho_{Ni} = 8.9$ g/cm^3, $\rho_{Ti} = 4.5$ g/cm^3). Furthermore, due to the narrow stoichiometric range of existence of the NiTi phase, the temperature of the martensitic transformation is strongly dependent on the chemical composition, and thus multiple re-melting is required to achieve the suitable homogeneity. The difficulties of working and mechanically machining NiTi also contribute to increase the production costs, thus limiting the commercial availability of this material.

For these reasons, the necessity of alternative methods for the fabrication of NiTi has become evident. Among synthetic techniques, powder metallurgy (PM) has been actively pursued as it provides a "near-net shape" processing method which avoids the costly VIM or VAR and the associated manufacturing steps. PM has the potential of producing a variety of component shapes while eliminating machining operations as well as avoiding the problems of casting defects due to segregation [17,18]. In this context, various powder synthesis routes have been investigated, such as reactive sintering [14] and hot-isostatic pressing [19].

In addition to the techniques mentioned above, self-propagating high-temperature synthesis (SHS) or combustion synthesis (CS) has advantages of time and energy savings that make it an attractive alternative to the conventional methods for the production of various classes of materials, including carbides, borides, nitrides, hydrides, intermetallics [17,18,20]. Also the possibility to form porous products is a well known feature of the SHS reactions. Due to the intrinsic characteristics of the technique, the porosity of SHS products derives both from the original porosity of the green pellet and from other sources typical of the synthesis process. These include the change in molar volume, the thermal migration resulting from the combustion front thermal gradients and, in particular, gas evolution due to the volatile impurity expulsion [21]. Porosity, mean pore size, and pore size distribution can moreover be controlled to a good extent in the SHS process. Porosity can be increased by either performing the reaction under reduced pressure or by adding a gasifying agent [22]. Pore size can be controlled by varying the reaction temperature through the addition of diluents to the initial mixture (generally the same reaction product) [20]. When homogeneous porosity is desired, great care must be paid to the ignition step to avoid non-uniform temperature profiles within the sample. Short ignition times are therefore required; mechanical activation of the reactants (MASHS) has been proven to greatly reduce ignition time and temperature in many combustion reactions [23–25].

Several works concerning the preparation of porous NiTi by combustion reactions have been reported, in which typically reactions have been conducted in two different modes: (a) SHS when the reaction initiates locally in a small volume and propagates from one side to the other side of the sample [6–8,13,14,26–30], and (b) volume combustion [27,31,32], when the entire sample is heated up to the ignition temperature and the chemical process starts at the same time throughout the entire pellet. With the exception of the noticeable work of Biswas [31] in which single phase porous NiTi was prepared by a modified volume combustion route, most of the works concern the SHS mode. NiTi samples prepared by SHS were shown to have a porosity above 50% [6,7,13,26] with a high fraction of interconnected pores; reactants particle size, reactant mixing procedure and initial green density have been varied to obtain ideal porosity content and shape.

Due to the relatively low exothermicity of the reaction ($\Delta H \approx 67$ kJ/mol) the synthesis of NiTi requires pre-heating of the sample to achieve self-sustained combustion [15]. Pre-heating temperature was shown to influence the amount of transient liquid phase present at the combustion front [7,13]. This ultimately controls the morphology of the product: excessive pre-heating has dramatic effect such as anisotropy in pore structure, formation of undesired macro-porosity and extended product melting [13].

The aim of the present study is an experimental (and parallel simulation) study of the combustion synthesis of porous Ni–Ti compounds, with particular attention to the effect of the heating and the ignition processes on the reaction phenomenon. As already said, due to the high thermal conductivity of reactants and products, ignition plays a critical role in the reaction and the product morphology. Markedly different reaction temperatures were observed by different authors [7,13] when conventional heating methods (e.g. tungsten coil) were used, due to the lack of control of the energy transfer intrinsically linked to these methods. Improvement made by using chemical igniters have been tried [7] but limited benefits were obtained. In the present study an integrated laser diode system has been used which allows to operate using short ignition times and a more careful control of the ignition conditions than conventional techniques. For a better understanding of experimental results, 0-D and 1-D numerical codes have been used to estimate some thermophysical properties of the pellets. The information obtained through simulation can as a matter of fact help in having a more detailed description of the thermal evolution of the ignition and the propagation characteristics of the SHS process.

2. Experimental apparatus and procedures

2.1. Combustion synthesis experiments

Samples have been prepared starting from elemental powders of Ni and Ti, homogeneously dry mixed in the stoichiometric ratio 1:1. Experiments with stoichiometric ratios Ni:Ti, 1:2 and 3:1 have also been performed for the ignition tests. The powders have then been cold pressed into two families of cylindrical pellets, the first one obtained by mixing

finer powders (particle size Ni = 3 μm, Ti < 45 μm) and the second one by mixing coarser powders (particle size Ni < 150 μm, Ti < 150 μm). All the tests have been carried out in a stainless steel combustion chamber (volume = 15 l) under a 0.7 bar Ar (99.98%) pressure by means of the apparatus depicted in Fig. 1. The key feature of our experimental apparatus is the compact integrated laser diode system (LW-30250) that delivers a maximum power of 250 W in continuous wave mode with a wavelength centred at 805–810 nm. Laser power is delivered via an optical fibre bundle that can be focused on different spot diameters and distances. These laser features permit, by a movement system (2-axis micro-translator) where the laser head is placed, to easily collimate the vertical axis of the sample with the laser beam and to drive, by a PC, the intensity and time duration of the power deposited on the sample. The combustion temperature has been acquired by a two-colour pyrometer (Micron fibre optic model M78) with a response time of 40 ms, focused on the middle of the sample. Moreover, in order to verify the accuracy of the two-colour pyrometer measurement, a thermocouple (Pt/Pt–10%Rh, bead size 127 μm and response time of about 10 ms), placed in the sample during the compaction of the reactant powders, has been used. The combustion front propagation rate has been determined from the images of the reaction front position, video-recorded by a TV camera system (Chugai Boyeki Co. YCH19), and the time superimposed on the video images by using a time code generator. Pre-heating of the samples was obtained by inserting the pellets in a home-made heating holder with some holes for the regression rate and temperature measurements (Fig. 2). By using this equipment, the sample can be uniformly heated up to 600 °C and the temperature inside the heater can be continuously monitored by two thermocouples placed in two different points of the heater.

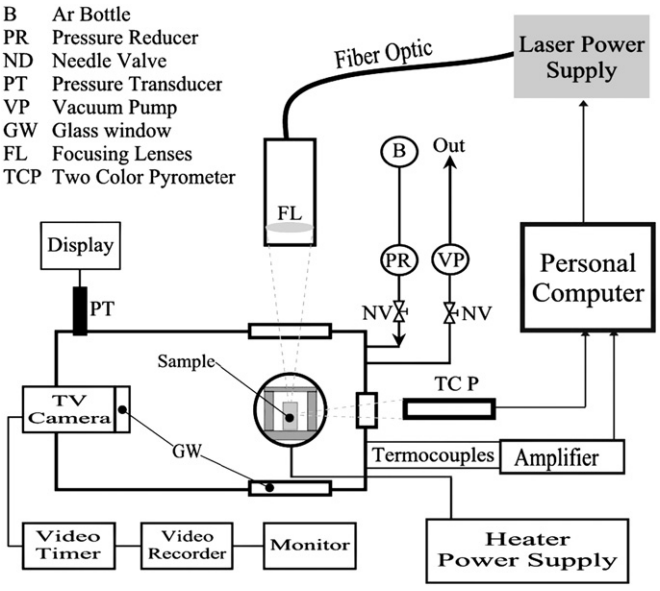

Fig. 1. Experimental apparatus scheme.

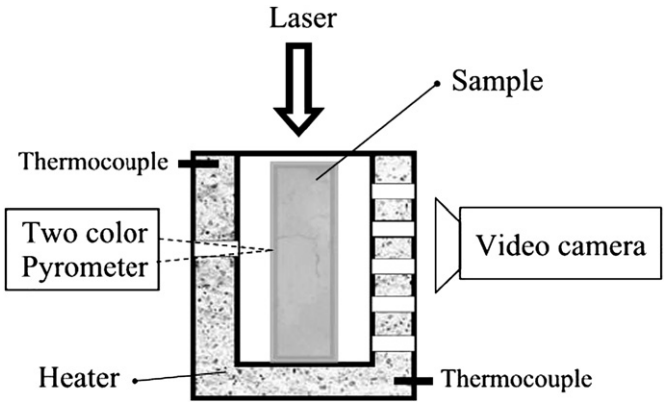

Fig. 2. Sample heater scheme.

Typically, experiments are performed by placing the sample inside the heater, and then increasing the sample temperature to its selected final value. This operation requires about 10 min (in order to reach the same temperature at the bottom and at the top side of the sample), but it guarantees that the ignition of the powder mixture occurs only when a uniform temperature distribution is reached in the whole sample. The sample is then ignited through a laser shot of 200–250 W for 0.3–0.8 s, and this condition permits to minimize changes in the temperature profile inside the sample. The laser shot duration was generally selected depending on the sample characteristics (porosity and thermal conductivity).

2.2. Ignition experiments

The investigation of the parameters controlling the ignition of the combustion reaction has been performed with a special experimental setup that was described in detail in a previous work [28]. Briefly, smaller samples with a diameter of 6 mm and an height of 0.5 ± 0.1 mm are suspended (holder should not touch the samples to minimize heat loss by conduction) by means of a thermocouple (Pt/Pt–10%Rh, bead size 127 μm) inserted in the middle of the sample and brought to thermal explosion condition by uniformly heating by the laser. Laser powers, ranging from 300 to 800 W/g, have been used to heat the samples up to the ignition temperature while higher laser powers as a matter of fact cause a too rapid increase in the sample temperature and ignition condition is reached when non-uniform distribution of temperature is present inside the sample. Moreover, fast heating rates (less than 5 s) sometimes make it difficult to correctly define the ignition temperature.

3. Results

An accurate study of the radiant energy contribution to the ignition and propagation processes requires the knowledge of the thermal conductivity ($K_c(T)$) of the reacting mixture and of the absorbance (α) of the surface irradiated by the laser. These data are necessary to define, for any experimental condition, the temperature distribution in the sample at the

ignition step. Without a consistent study of these two parameters, the experimental results concerning the heating, ignition transient and reaction cannot be quantitatively interpreted to give information such as the ignition energies. Moreover, $K_c(T)$ and α are required when numerical simulation of the ignition transient relevant to long samples are computed.

Concerning thermal conductivity of pressed powders, it can actually differ from the bulk value because of the porosity [33], and is one of the most relevant parameters in defining the combustion behavior [34]. Thermal conductivity evaluation is here based on the capability to heat the upper side of the sample, by laser energy, and then to measure the temperature evolution in time, by two thermocouples placed at a known distance, inside the pellet [35]. The same experimental temperature profiles have been numerically reproduced by the 1-D code [36], once the dependence of the thermal conductivity on porosity and temperature has been properly chosen. Fig. 3 shows the experimental temperature profiles (open circles) during a heating–cooling cycle as measured by two thermocouples placed on the upper surface and 3 mm below it. The data refer to a Ni:Ti, 1:1 mixture with a porosity of 33 vol% and to a laser power of 49.8 W cm^{-2}. From these data the thermal conductivity and its dependence on temperature could be evaluated and used to simulate temperature profiles at other positions inside the sample, as those reported on the same figure as dash-dotted lines. The dependence of effective thermal conductivity on porosity (from 34 to 66 vol%) and temperature is shown in Fig. 4 where data obtained by numerical simulations are reported. Comparisons between these data and the K_c values relevant to the full dense materials (porosity = 0%) indicate that high porosity strongly reduces the K_c values. Moreover, the dependence of K_c on porosity, depicted by the calculated curves (see formula reported in Fig. 4), was found to be much more significant than that on temperature in particular for the sample featured by high porosity values. The

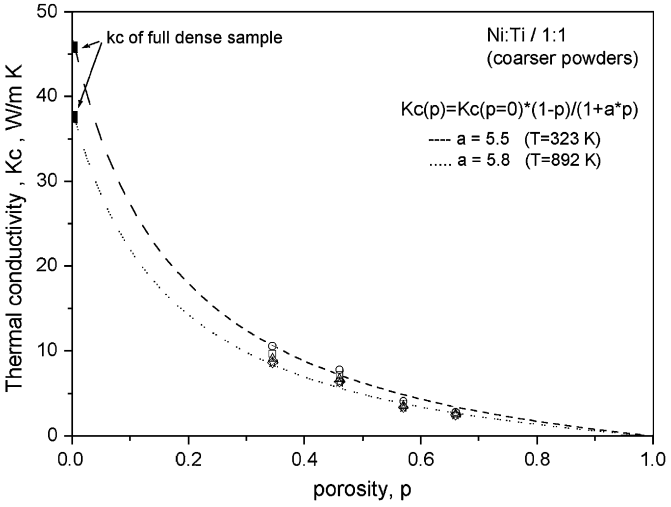

Fig. 4. Dependence of K_c on porosity at various temperatures. Symbols refer to experimental data, continuous lines to fitting curves. Sample composition Ni:Ti = 1:1.

radiant absorbance of the Ni:Ti, 1:1, 1:2, 3:1 powder mixtures has been, on the other hand, evaluated using the thin samples setup previously described (see Section 2.2). The signals, generated by the thermocouple during the heating and cooling transient, have been recorded and used to calculate α by the 0-D code simulation [28]. The code simulates a volumetric heating of the sample (thermal explosion mode). For this reason, 1-D code simulations were used to determine the minimum heating time for the temperature difference between the top and bottom surfaces of the sample to be below 1% at the ignition temperature (in this case, about 900 °C). The results, reported in Fig. 5 for various laser powers, indicate that this condition is fulfilled for heating times above 5 s.

Experiments aimed at the estimation of the sample radiant absorbance were performed for the two different powder

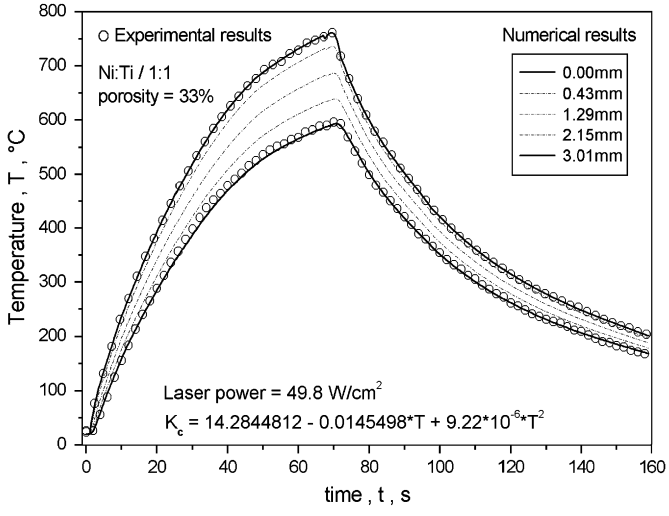

Fig. 3. Temporal evolution of temperature at different positions inside the sample irradiated on the top surface by a laser power of 49.8 W cm^{-2}; open circles refer to experimental data, dash-dotted lines to simulation data. Sample composition Ni:Ti = 1:1, porosity 33%.

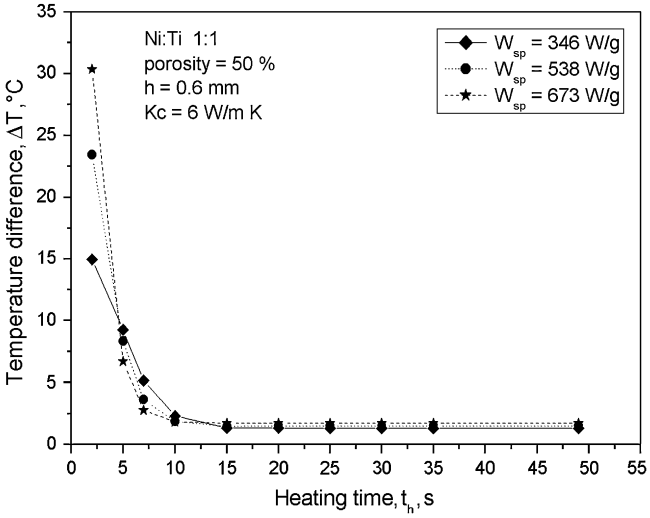

Fig. 5. Temporal evolution of the temperature difference between the upper and lower surface of small samples for different laser powers.

batches (finer and coarser) and the three different stoichiometries. Results are summarized in Table 1 that indicates the average value of α obtained by simulations of the heating sample process up to the ignition temperature.

Even though it is difficult to compare radiant absorbance results since it strongly depends on surface roughness, porosity distribution, particle sizes, particle hardness and compression procedure, it can be observed that a much higher α is obtained when a shorter laser wavelength is used, as in our setup, than those obtained by using a CO_2 laser system [27], previously employed in several SHS studies. This represents a noteworthy advantage when short ignition times are required and helps in reducing the uncontrolled pre-heating of the reacting pellet. In general it can be also observed that the compositions richer in Ni have larger absorbance due to the higher rigidity and hardness of Ni with respect to Ti which ultimately leads to a higher surface roughness. Surface roughness and consequently α are also higher when coarser powders are used.

3.1. Ignition

The capability to reach the ignition condition by the reacting pellet is influenced both by parameters belonging to the pellet (K_c, α, porosity, ΔH, grain sizes) and by the heating cycle [31]. For that reason experiments were conducted in which the following parameters were varied: (a) stoichiometry of the reacting mixture (Ni:Ti, 1:1, 1:2 and Ni:Ti, 3:1), (b) particle size of the reactants, (c) heating transient (with particular attention to its final stages where temperature varies between 800 °C and the ignition temperature).

Data are reported in the following in terms of absorbed power normalized to the relevant sample mass m:

$$W_{sp} = \frac{\alpha W_o w_a}{m} \quad (1)$$

where α is the radiant absorbance of the sample, W_o the nominal power emitted by the laser and w_a (90%) the transmittance of the reactor chamber window. Pictures depicting the simplest heating transient, where the laser power is kept constant during the whole test, are shown Fig. 6 for a sample of composition Ni:Ti, 1:1. The corresponding temperature trace, recorded by the thermocouple holding the sample (porosity equal to 57%) heated by a laser power of 647 W/g is shown Fig. 7 together with the temperature simulated with our 0-D code. After ignition ($T = 925$ °C), the pellet temperature rises abruptly, due to the exothermic reactions, and reaches its maximum value.

Table 1
Surface absorbance (α) of pellets with different compositions and particle sizes (C = coarse, F = fine)

Powder stoichiometry	α	α [29]
	$\lambda = 0.81$ μm	$\lambda = 10.6$ μm
Ni:Ti 1:1 C	0.555	0.130
Ni:Ti 1:1 F	0.523	–
Ni:Ti 3:1 C	0.660	0.110
Ni:Ti 3:1 F	0.603	–
Ni:Ti 1:2 C	0.565	0.118
Ni:Ti 1:2 F	0.510	–
Ni[a]	0.410	0.020
Ti[a]	0.485	0.150

Left column refers to the integrated laser diode system; right column refers to a CO_2 laser system.
[a] Surface polished [37].

In Table 2 selected tests are reported to indicate the effect of the above listed parameters on the ignition temperature, ignition time, and ignition energies (for the ignition energies calculation see for instance Refs. [27–30]). Moreover, the main results can be summarized as follows.

- Ignition temperatures range between ~870 and ~1070 °C, depending on the experimental conditions, while ignition energies vary between ~21 and ~31 kJ/mol of atoms. Differently from several SHS reactions involving metals, in which the ignition temperature equals the melting point of the low-melting point component [27], in the Ni–Ti system the ignition temperature is well below the melting point of both reactants. The measured temperatures, on the other hand, approximately correspond to two important features of the Ni–Ti phase diagrams that can be addressed as responsible for the ignition of the combustion reaction: maximum solubility of Ni in β-Ti (≈9 wt% of Ni in β-Ti at 942 °C) and lowest temperature eutectic (942 °C) (24 at.% Ti) [38]. This is in agreement with the DTA results reported by Biswas [31] who identified two exothermic peaks, one at ~850 °C and the other at ~950 °C. The low temperature corresponded to solid-state diffusion reaction that preceded the ignition, while the higher temperature one corresponded to the liquid formation at the eutectic temperature and is the main factor responsible for the sample ignition and reaction.
- The parameter that mostly affects the ignition temperature was found to be the heating transient features. Typical heating cycles are reported in Figs. 8 and 9, in which heating of the sample is performed by delivering the heating power in a stepped way. As the number of steps increases (and consequently heating times also increase) the ignition temperatures are shifted to higher values. The increase in ignition temperature is caused by the product formation at the grain interface which also causes a decrease in the following combustion energy as it partially consumes the reactants [31]. Consequently the post-combustion exothermic peak (see Figs. 7–9) decreases with ignition time. This result opens the possibility for a fine control of the ignition and the combustion peak temperature by acting on the laser power cycle.
- Even though not investigated in a quantitative systematic way (only two different commercial sets of powder were used), the increase of reactant particle size was observed to moderately (~50 °C) increase the ignition temperature. A similar dependence was found in many other SHS systems as a consequence of the increased surface contact area between finer reactants [27–30].

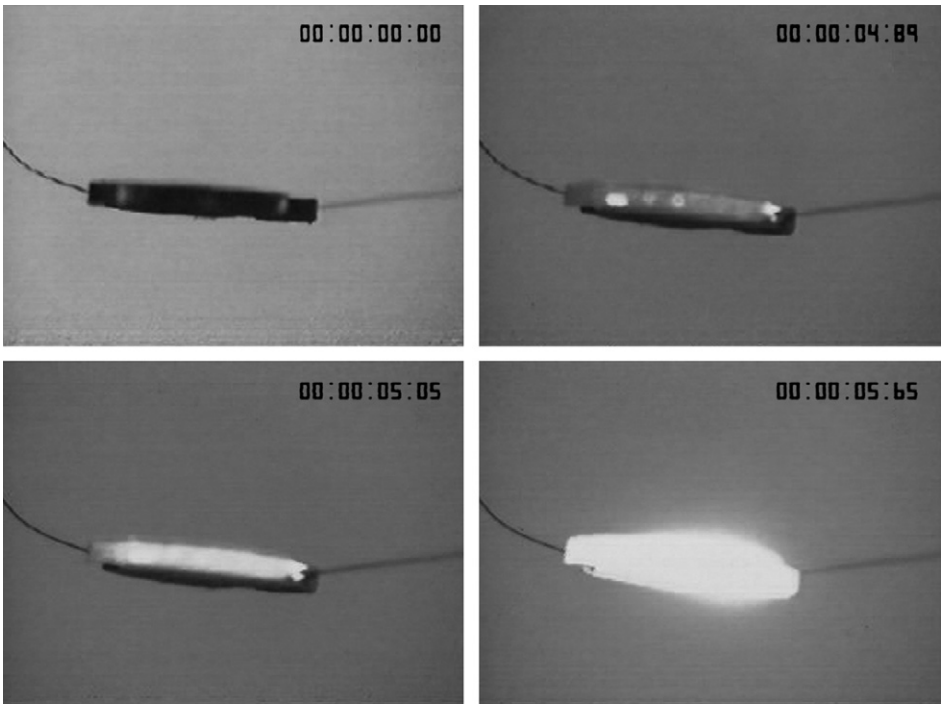

Fig. 6. Photographic sequence of the ignition of small samples.

- Ni:Ti, 1:1 and Ni:Ti, 1:2 compositions were found to ignite at almost identical temperatures (and energies) while Ni:Ti, 3:1 was observed to ignite at slightly higher temperatures, when similar heating cycles were used. The sample stoichiometry is indeed the most difficult variable to interpret since it controls not only the reaction enthalpy but also thermal conductivity and the radiant absorbance of the surface (see Table 1). Indeed the similarity of the ignition temperature is in support of the fact that an identical chemical step (eutectic liquid formation) is responsible for ignition.

Finally it was necessary to ascertain if the ignition parameters obtained in the thermal explosion mode on small samples could be valid also in the case of SHS performed on conventional cylindrical samples. Ignition temperature of the long pellets was measured by placing the thermocouple on the top surface of the pellet topped by a thin layer of graphite powder pressed all together. In this way uniform temperature distribution could be obtained. A typical result (sample length 13 mm, diameter 8 mm, no pre-heating process) is shown in Fig. 10 for a reaction starting at the temperature of 920 °C; this value is close to that obtained with the small sample in the same experimental condition (916 °C).

3.2. Combustion synthesis

The demand for uniform morphology of the product (in particular as far as pore size and pore size distributions are concerned) requires a delicate control of the ignition conditions in order to avoid non-uniform temperature distribution within the reacting pellet, which is caused by the finite duration of the laser pulse. So far, this aspect has been largely overlooked in the SHS literature; the ignition is actually most frequently accomplished though an electrically heated element which prevents a careful control of the ignition parameters. This drawback is particularly severe when dealing with metallic samples (as in our case), due the high thermal conductivity of the pellet. Moreover, the Ti–Ni system shows a relatively low exothermicity and therefore requires some degree of pre-heating in order to establish steady state propagation on the one hand, and relatively long ignition times on the other.

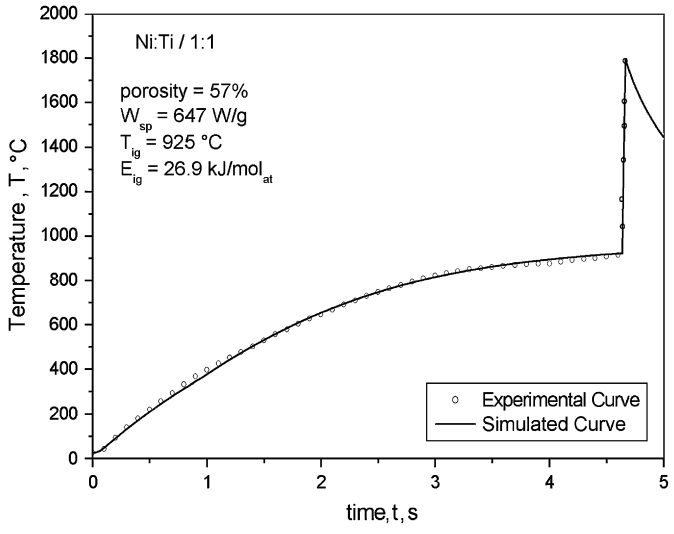

Fig. 7. Experimental (symbols) and simulation (line) temperature evolution of a Ni:Ti = 1:1 small sample heated with a constant laser power.

Table 2
Ignition temperature (T_{ig}), ignition time (t_{ig}) and ignition energy (E_{ig}) as a function of heating power (W_{sp}), composition and particle size (C = coarse, F = fine)

Ni:Ti	W_{sp} (W/g)	t_{ig} (s)	T_{ig} (°C)	E_{ig} (kJ/mol$_{at}$)
1:1 C	525	4.95	916	26.4
1:1 C	450-650	47.4	1020	30.0
1:1 F	448	8.0	877	24.9
1:1 F	428-571	57.2	1039	27.5
1:2 C	432	7.60	914	26.3
1:2 C	514-543	21.45	947	26.0
1:2 F	690	3.02	855	24.8
1:2 F	395-416	23.44	890	25.1
3:1 C	566	3.30	925	26.5
3:1 C	510	5.58	997	26.6
3:1 F	750	2.64	925	26.5
3:1 F	425	9.88	956	26.9

Pre-heating can be performed (and often in the SHS literature) by lengthening the duration of the ignition source (either laser or heating coils); an example of such method is reported in Fig. 11, where the sample was pre-heated through a low power laser pulse (40 W cm^{-2}) for 230 s and successively ignited through a high power pulse of short duration (400 W cm^{-2}, 0.3 s). When pre-heating is conducted in this way fairly steep temperature profiles build up inside the pellets. The temperature profile inside the reacting pellet generated by the laser energy absorbed during the laser shot was simulated (1-D code) for various times as shown in Fig. 12. As a consequence, once the reaction has ignited, both combustion temperature and wave velocity are not constant in space as shown in Fig. 13 where the variation of the propagating front velocity (as measured by video recordings of the reaction) as a function of the distance from the top surface is presented.

To avoid a non-uniform temperature profile within the samples a controlled-temperature profile must be properly chosen. This was done by placing the sample inside the home-made heater of Fig. 2 and increasing the whole pellet temperature to selected values. By means of controlled pre-heating, considerably shorter laser pulses can be used, which in turns, means minimizing the temperature non-homogeneities inside the pellet. For instance, using a pre-heating temperature of 300 °C and sample porosity of 50%, it was possible to ignite the sample by a laser power shot of 200 W impinging on the sample for 0.3 s. Moreover, thanks to the pre-heating procedure steady state propagation of the front was observed.

Finally, following this procedure, tests were carried out on the Ni:Ti, 1:1 composition choosing different pre-heating temperatures and the results relative to combustion temperature and wave velocities are depicted in Fig. 14.

In these tests wave velocity values with an error of ±5% and temperatures with an error of ±3% have been obtained.

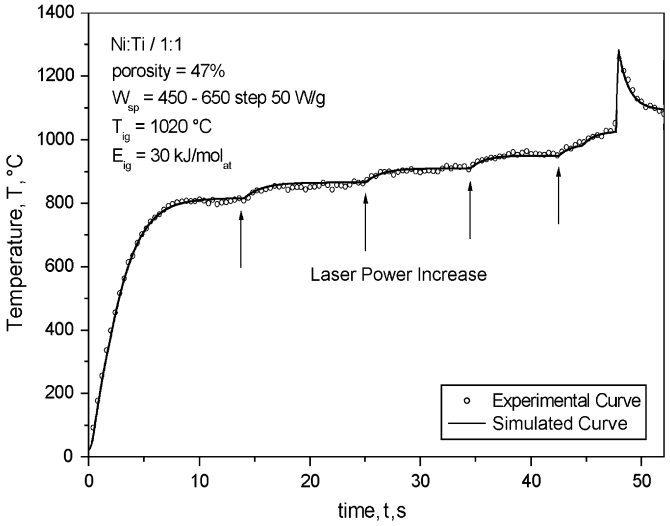

Fig. 9. Experimental (symbols) and simulation (line) temperature evolution of a Ni:Ti = 1:1 small sample heated with a five steps laser power.

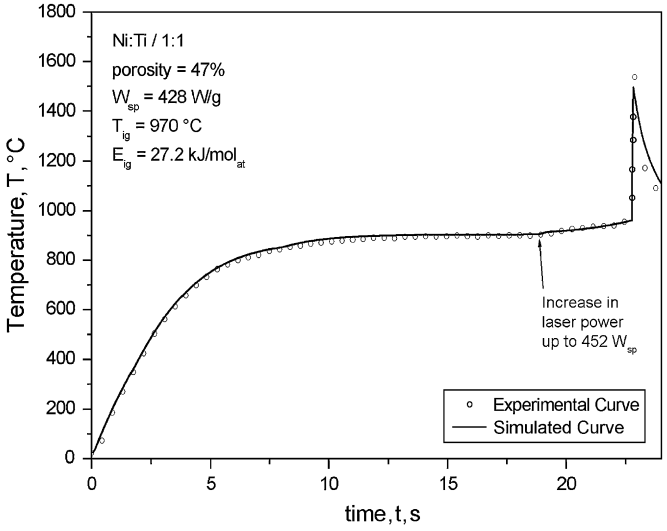

Fig. 8. Experimental (symbols) and simulation (line) temperature evolution of a Ni:Ti = 1:1 small sample heated with a two steps laser power.

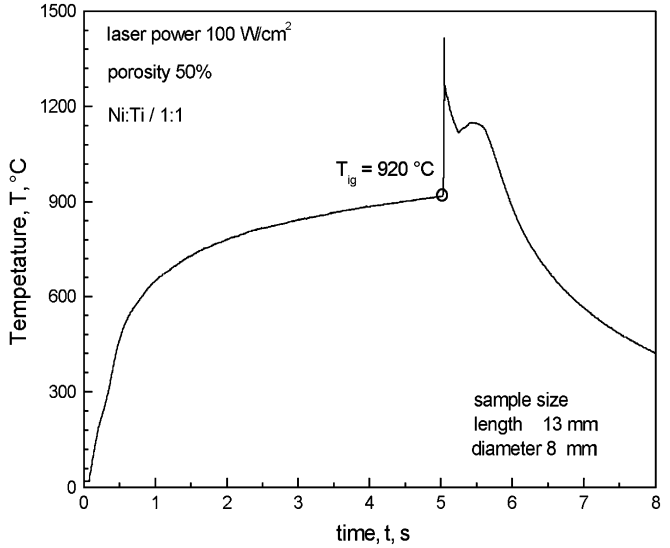

Fig. 10. Experimental temperature evolution of a Ni:Ti = 1:1 long sample heated with a constant laser power.

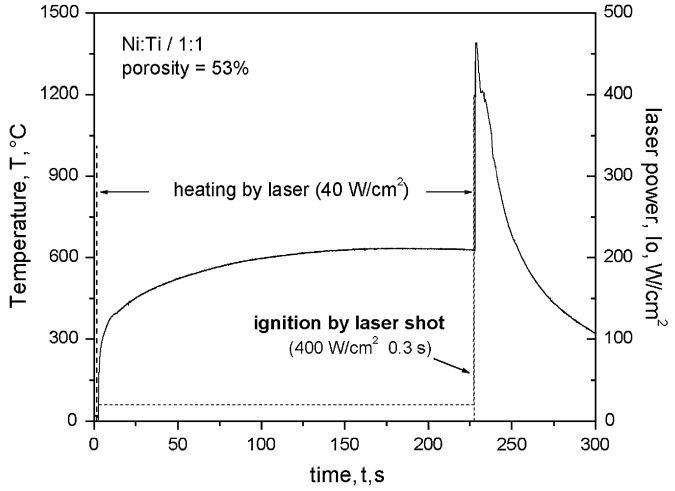

Fig. 11. Experimental temperature evolution of a Ni:Ti = 1:1 long sample pre-heated from the top surface with 40 W cm^{-2} laser pulse for 230 s and then ignited with 400 W cm^{-2} pulse.

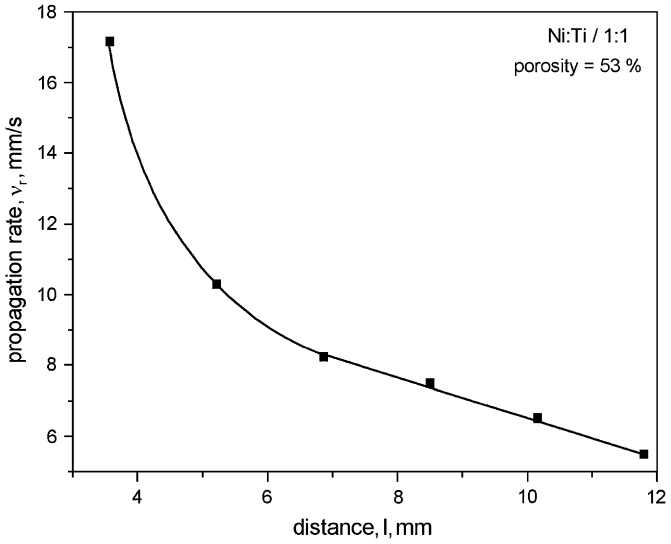

Fig. 13. Variation of the combustion front velocity along the sample tested under conditions reported in Fig. 11.

As a consequence of pre-heating the measured reaction temperatures (measured by pyrometer averaging the temperature value on a spot size of 2 mm and micro-thermocouples inserted in the middle of the sample) are higher (~1450 °C) than the calculated adiabatic temperature (1165 °C) and also exceed the melting temperature of the NiTi (1310 °C). The latent heat of fusion produced minimizes the effect of pre-heating on the combustion temperature while more pronounced is the effect on velocity. In agreement with previous literature results [16,31] the product contained NiTi as the main component with minor amounts of $NiTi_2$ and Ni_3Ti.

4. Conclusions

The ignition of self-propagating reactions in the Ni–Ti system has been investigated using an integrated experimental simulation approach. Experiments have been conducted using an integrated laser diode system which allows to carefully control the heating process and, in such a way, to reach different ignition conditions.

Thermal conductivity ($K_c(T)$) and absorbance (α) of the samples with different compositions, porosities and reactant particle sizes were measured and their values were used to simulate thermal profiles inside the pellets and to calculate ignition energies.

Ignition temperatures, times, and energies for compositions Ni:Ti = 1:1, 1:2, and 3:1 strongly depend on the heating cycle, while a less pronounced dependence on composition and reactant particle size was observed. Minimum ignition temperatures were found to correspond to the maximum solubility of Ni in β-Ti and to the lowest eutectic (942 °C).

An experimental procedure that combines controlled pre-heating of the sample through an external furnace and very

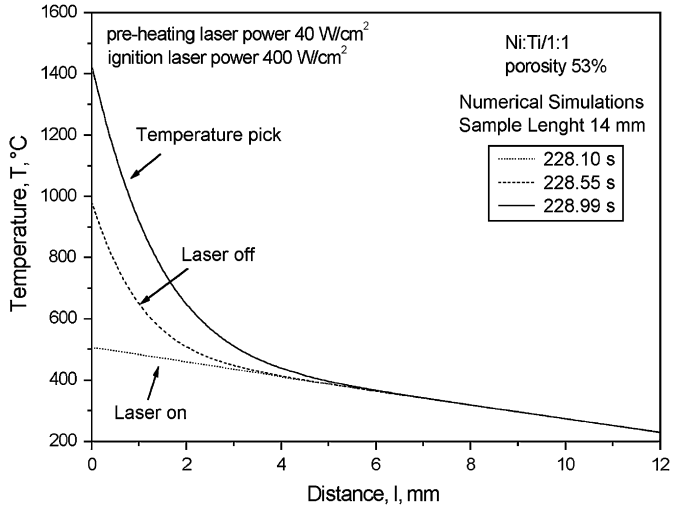

Fig. 12. 1-D simulation of the temperature profile inside the sample tested under conditions reported in Fig. 11.

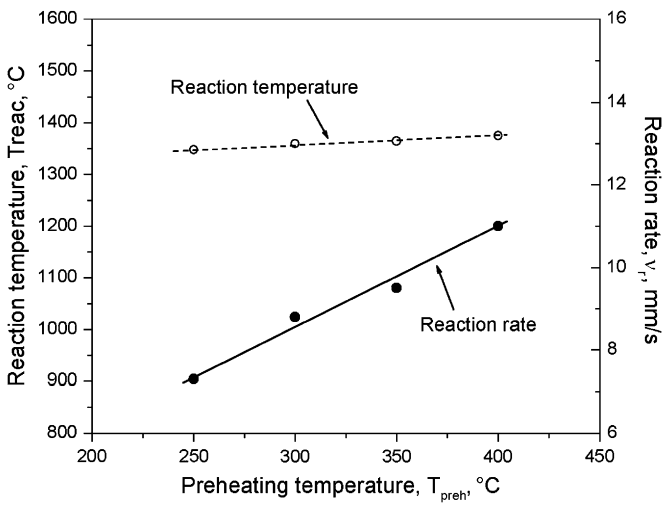

Fig. 14. Dependence of the combustion front velocity and temperature on controlled pre-heating temperatures.

short laser shots was shown to minimize temperature gradients inside the pellet during the heating and ignition transient. Consequently, steady state propagation front with constant temperature and velocity throughout the entire sample was observed, which constitute a noteworthy improvement in comparison to conventionally ignited reactions.

Acknowledgements

The authors are grateful to master student S. Squaranti (Department of Aerospace Engineering, Politecnico of Milano) for carrying out experiments in the IENI-CNR labs during the preparation of his thesis.

References

[1] Lipscomb IP, Nokes LDM. The application of shape memory alloys in medicine. Suffold: Mechanical Engineering Publications Limited; 1996.
[2] Bekker A, Brinson LC. Acta Mater 1998;46:3649.
[3] Inaekyan KE, Prokoshkin SD, Brailovski V, Khmelevskaya IYu, Demers V, Dobatkin SV, et al. Mater Sci Forum 2006;503:597.
[4] Otsuka K, Ren XB. Intermetallics 1999;7:511.
[5] Chu CL, Chung CY, Lin PH, Wang SD. J Mater Process Technol 2005;169:103.
[6] Li B-Y, Rong L-J, Li Y-Y, Gjunter VE. Intermetallics 2000;8:881.
[7] Chu CL, Chung CY, Lin PH. Mater Sci Eng A 2003;366:114.
[8] Chung CY, Chu CL, Wang SD. Mater Lett 2003;58:1683.
[9] Yeh CL, Sung WY. J Alloys Compd 2003;376:79.
[10] Gjunter VE. Delay law and new class of materials and implants in medicine. Northampton: SST; 2000.
[11] Simske SJ, Sachdeva RLC. J Biomed Mater Res 1995;29:527.
[12] Li B-Y, Rong L-J, Li Y-Y, Gjunter VE. J Mater Res 2000;15:10.
[13] Li B-Y, Rong L-J, Li Y-Y, Gjunter VE. Acta Mater 2000;48:3895.
[14] Li B-Y, Rong L-J, Li Y-Y, Gjunter VE. Intermetallics 2000;8:643.
[15] Li B-Y, Rong L-J, Li Y-Y. Scripta Mater 2001;44:823.
[16] Locci AM, Orrù R, Cao G, Munir ZA. Intermetallics 2003;11:555.
[17] Moore JJ. Prog Mater Sci 1995;39:243.
[18] Moore JJ. Prog Mater Sci 1995;39:275.
[19] Yuan B, Chung CY, Zhu M. Mater Sci Eng A 2004;382:181.
[20] Munir ZA, Anselmi-Tamburini U. Mater Sci Rep 1989;3:277.
[21] Munir ZA. J Mater Synth Process 1993;1:387.
[22] Hunt EM, Pantoya ML, Jouet RJ. Intermetallics 2006;14:620.
[23] Gras C, Gaffet E, Bernard F. Intermetallics 2006;14:521.
[24] Anselmi-Tamburini U, Maglia F, Doppiu S, Monagheddu M, Cocco G, Munir ZA. J Mater Res 2004;19:1558.
[25] Maglia F, Anselmi-Tamburini U, Deidda C, Delogu F, Cocco G, Munir ZA. J Mater Sci 2004;39:5227.
[26] Chu CL, Chung CY, Lin PH. J Mater Sci 2004;39:4949.
[27] Zanotti C, Giuliani P. Propell Explos Pyrot 2004;29:112.
[28] Monagheddu M, Bertolino N, Giuliani P, Zanotti C, Anselmi Tamburini U. J Appl Phys 2002;92:594.
[29] Bertolino N, Monagheddu M, Tacca A, Giuliani P, Zanotti C, Anselmi Tamburini U. Intermetallics 2002;11:41.
[30] Galfetti L, Zanotti C, Giuliani P. Radiant heating and ignition of solid propellants. In: Wrobel LC, et al., editors. Advanced computational methods in heat transfer II. Natural/forced convection and combustion simulation, vol. 2. Boston: Elsevier Applied Science; 1992. p. 613–32.
[31] Biswas A. Acta Mater 2005;53:1415.
[32] Vilyunov VN, Zarko VE. Ignition of solids. Amsterdam: Elsevier Science Publishers; 1989.
[33] Miura S, Terada Y, Suzuki T, Liu CT, Mishima Y. Intermetallics 2000;8:151.
[34] Gennari S, Maglia F, Anselmi-Tamburini U, Spinolo G. Intermetallics 2003;11:1355.
[35] Zanotti C, Riva G, Giuliani P, Daminelli G. Characterization of thermal protection systems used for space applications. CNR technical report IENI/N. R-2005/; 2005.
[36] Muolo ML, Ferrera E, Morbelli L, Zanotti C, Passerone A. In: Ninth international symposium on materials in a space environment. ESA SP-540 proceedings book. Noorwijk; 2003. p. 467–72.
[37] Sala A. Radiant properties of materials. Warsaw: Elsevier Book, PWN-Polish Scientific Publishers; 1986.
[38] Binary phase diagrams. Metals Park, OH, USA: American Society for Metals; 1986. p. 1978.